Standard Model thermodynamics across the electroweak crossover

JCAP07(2015)035

(http://iopscience.iop.org/1475-7516/2015/07/035)

Journal of Cosmology and Astroparticle Physics
An IOP and SISSA journal

Standard Model thermodynamics across the electroweak crossover

M. Laine and M. Meyer

Institute for Theoretical Physics, Albert Einstein Center, University of Bern, Sidlerstrasse 5, CH-3012 Bern, Switzerland

E-mail: laine@itp.unibe.ch, meyer@itp.unibe.ch

Received March 23, 2015
Accepted June 23, 2015
Published July 22, 2015

Abstract. Even though the Standard Model with a Higgs mass $m_H = 125\,\mathrm{GeV}$ possesses no bulk phase transition, its thermodynamics still experiences a "soft point" at temperatures around $T = 160\,\mathrm{GeV}$, with a deviation from ideal gas thermodynamics. Such a deviation may have an effect on precision computations of weakly interacting dark matter relic abundances if their mass is in the few TeV range, or on leptogenesis scenarios operating in this temperature range. By making use of results from lattice simulations based on a dimensionally reduced effective field theory, we estimate the relevant thermodynamic functions across the crossover. The results are tabulated in a numerical form permitting for their insertion as a background equation of state into cosmological particle production/decoupling codes. We find that Higgs dynamics induces a non-trivial "structure" visible e.g. in the heat capacity, but that in general the largest radiative corrections originate from QCD effects, reducing the energy density by a couple of percent from the free value even at $T > 160\,\mathrm{GeV}$.

Keywords: particle physics - cosmology connection, cosmological phase transitions

ArXiv ePrint: 1503.04935

doi:10.1088/1475-7516/2015/07/035

JCAP07(2015)035

Contents

1 Introduction 1

2 Basic setup 2

3 Master equation 3

4 Effects from scale violation by quantum corrections 4

5 Effects from the Higgs condensate 5
- 5.1 Outline 5
- 5.2 Perturbative contributions 6
- 5.3 Non-perturbative contribution 7
- 5.4 Combined expression 8

6 Vacuum subtraction and renormalization 9

7 Phenomenological results 10

8 Conclusions 12

A 3d condensate in perturbation theory 13

B Differences with respect to ref. [18] 14

1 Introduction

The excellent performance of the Standard Model (SM) in describing LHC data suggests that the SM represents a precise description of nature up to energy scales of several hundred GeV. If this observation continues to be confirmed by future runs, one consequence is that the Higgs phenomenon set in smoothly, i.e. without a phase transition, as the Universe cooled down to temperatures below 160 GeV [1]–[4] (cf. ref. [5] for a review of refined investigations). This would mean that the bulk motion of the plasma did not depart from thermal equilibrium and therefore did not generate cosmological relics.

Nevertheless, the thermodynamics of the SM could still have left a "background" imprint on other non-equilibrium physics that just happened to be going on. One example is that the B+L violating rate switched off rapidly around the crossover [6], and therefore determined which fraction of a given lepton number being produced around these temperatures could be converted into baryons (cf. e.g. ref. [7]). Another is that if Dark Matter particles decoupled at around this period, even small features in the equation of state could have had an impact [8]. (Similar considerations can be carried out for the QCD crossover, cf. refs. [9, 10] and references therein.) A rough estimate for the decoupling temperature of weakly interacting particles of mass M is $T \sim M/25$, so that we may expect the largest sensitivity for $M \sim 4\,\mathrm{TeV}$ or so.

The purpose of our study is to estimate the equation of state of the SM around the electroweak crossover. We do this through perturbative computations extending up to 3-loop level, as well as by making use of existing lattice simulations within a dimensionally

JCAP07(2015)035

reduced effective theory. Only the temperature is treated as a non-trivial canonical variable, with chemical potentials associated with conserved charges such as the baryon minus lepton number or the hypercharge magnetic flux set to zero.

The paper is organized as follows. After defining the basic observables in section 2, we derive a "master equation" in section 3 which relates the trace of the expectation value of the energy-momentum tensor to three ingredients. The first ingredient, scale violations through quantum corrections, is addressed in section 4. The second ingredient, the expectation value of the Higgs condensate, needs to be evaluated up to the non-perturbative level, and this is achieved in section 5. The third ingredient is related to vacuum renormalization and is discussed in section 6. All ingredients are put together in section 7, where we also present phenomenological results. Section 8 contains some conclusions as well as a discussion of the theoretical uncertainties of the current analysis. Readers not interested in technical details may start from section 7.

2 Basic setup

We consider the Standard Model with a Higgs potential of the form

$$\delta\mathcal{L}_{\mathrm{E}} = -\nu_{\mathrm{B}}^2\phi^\dagger\phi + \lambda_{\mathrm{B}}(\phi^\dagger\phi)^2\,, \tag{2.1}$$

where ν_{B}^2, λ_{B} are bare parameters (the corresponding renormalized parameters are denoted by ν^2, λ), and $\mathcal{L}_{\mathrm{E}}$ is a Euclidean (imaginary-time) Lagrangian. Denoting by $g^2 \in \{\lambda, h_t^2, g_1^2, g_2^2, g_3^2\}$ a generic coupling constant,[1] we concentrate on the parametric temperature range

$$T^2 \gtrsim \frac{\nu^2}{g^2} \tag{2.2}$$

in the following. At the lower edge of this range, the effective Higgs mass parameter of the dimensionally reduced theory [11, 12], $\bar{m}_3^2$ [13], is assumed to satisfy

$$|\bar{m}_3^2| \sim \left|-\nu^2 + g^2T^2\right| \lesssim \frac{g^3T^2}{\pi}\,, \tag{2.3}$$

but it can have either sign. If it is negative, we may expect to find ourselves in a "Higgs phase". Within a gauge-fixed perturbative treatment, this would imply that the Higgs field has an expectation value $v^2 \sim -\bar{m}_3^2/\lambda > 0$. Within the range of eq. (2.3), only relatively small expectation values $v \lesssim g^{\frac{1}{2}}\,T$ can be considered, where we counted $\lambda \sim g^2$.

It is well known that when momenta in the range $|\bar{m}_3^2| \sim (g^2T/\pi)^2$ are considered, which is a special case of eq. (2.3), then the dynamics of the system is non-perturbative [14, 15]. Therefore the dynamics needs to be treated with lattice methods. However, non-perturbativity is associated with particular modes only, and can be captured with a dimensionally reduced effective description [11, 12]. Even though the construction of this theory is perturbative, we expect to obtain a description accurate on the percent level within a weakly coupled theory such as the SM. This estimate is based on analyzing the influence from higher-order operators that are truncated from the dimensionally reduced theory (cf. section 5.4 of ref. [13]) and, more concretely, from a comparison of non-perturbative results for the location of the endpoint in the phase diagram of an SM-like theory based on the dimensionally reduced description and on direct 4-dimensional lattice simulations [16, 17]. (It would be interesting to repeat the latter type of a comparison for the physical value of the Higgs mass.)

[1] Here h_t denotes the top Yukawa coupling and g_1, g_2, g_3 are the gauge couplings related to the Standard Model gauge groups $\mathrm{U_Y}(1)$, $\mathrm{SU_L}(2)$ and $\mathrm{SU_C}(3)$.

JCAP07(2015)035

The basic observable that we consider is the thermodynamic pressure of the SM. The pressure can formally be defined through the grand canonical partition function $\mathcal{Z}$ as

$$\mathcal{Z} \equiv \exp\left(\frac{p_{\rm B}(T)V}{T}\right), \tag{2.4}$$

where the thermodynamic limit $V \to \infty$ is implied, and $p_{\rm B}$ denotes the bare result. The computation of $p_{\rm B}$ has previously been considered in ref. [18] for the case $\bar{m}_3^2 \sim g^2T^2$, and in ref. [19] for $\bar{m}_3^2 \sim g^3T^2/\pi$. Following refs. [18, 19][2] (which were inspired by ref. [20]) we write

$$p_{\rm B}(T) = p_{\rm E}(T) + p_{\rm M}(T) + p_{\rm G}(T)\,, \tag{2.5}$$

where $p_{\rm E}$ collects contributions from the momentum scale $k \sim \pi T$, $p_{\rm M}$ those from $k \sim gT$, $p_{\rm G}$ those from $k \sim g^2T/\pi$. Rephrasing terminology often used in the QCD context, we refer to the effective theory contributing to $p_{\rm M}$ as ESM ("Electrostatic Standard Model") and to that contributing to $p_{\rm G}$ as MSM ("Magnetostatic Standard Model").

As defined by eq. (2.4) the pressure is ultraviolet divergent. We renormalize it by assuming that the pressure (and energy density) vanish at $T = 0$. The renormalized pressure can then be written as

$$p(T) \equiv p_{\rm B}(T) - p_{\rm B}(0)\,. \tag{2.6}$$

Our goal is to determine the dimensionless functions $p(T)/T^4$ and $T\partial_T\{p(T)/T^4\}$ up to $\mathcal{O}(g^5)$. For the latter quantity, it turns out that the contribution of the softest momentum modes needs to be treated non-perturbatively in order to reach this precision.

3 Master equation

Consider a normalized form of eq. (2.6), $p/T^4 = [p_{\rm B}(T) - p_{0\rm B}]/T^4$, where $p_{0\rm B} \equiv p_{\rm B}(0)$ denotes the bare zero-temperature pressure. Unless stated otherwise ultraviolet divergences are treated through dimensional regularization. In the difference of eq. (2.6) all $1/\epsilon$ poles cancel, so that the bare expressions can be replaced with renormalized expressions in the $\overline{\rm MS}$ scheme ($p_{\rm B} \to p_{\rm R}$, $p_{0\rm B} \to p_{0\rm R}$):

$$\frac{p(T)}{T^4} = \frac{p_{\rm R}(T;\bar{\mu},\nu^2(\bar{\mu}),g^2(\bar{\mu})) - p_{0\rm R}(\bar{\mu},\nu^2(\bar{\mu}),g^2(\bar{\mu}))}{T^4}\,. \tag{3.1}$$

Here $\bar{\mu}$ denotes the $\overline{\rm MS}$ renormalization scale.

We envisage that at some temperature ($T = T_0$) on either side of the crossover, say $T_0 \ll 160\,\mathrm{GeV}$ or $T_0 \gg 160\,\mathrm{GeV}$ so that $|\bar{m}_3^2| \gtrsim g^3T^2/\pi$, p/T^4 can be determined by a direct perturbative computation. The task then is to integrate p/T^4 across the electroweak crossover:

$$\frac{p(T_1)}{T_1^4} - \frac{p(T_0)}{T_0^4} = \int_{T_0}^{T_1}\frac{{\rm d}T}{T} \times T\frac{\rm d}{{\rm d}T}\left\{\frac{p(T)}{T^4}\right\}. \tag{3.2}$$

So, we need to compute the logarithmic temperature derivative of the dimensionless ratio p/T^4. The result is non-zero because of the breaking of scale invariance, either by the explicit mass term ν^2, or by quantum corrections related to running couplings.

[2] We agree with most of the results in these papers, however disagree with the renormalization condition for p and with certain technical details, cf. appendix B.

JCAP07(2015)035

Making use of standard thermodynamic relations, we note that

$$T\frac{\mathrm{d}}{\mathrm{d}T}\left\{\frac{p(T)}{T^4}\right\} = \frac{e(T)-3p(T)}{T^4} \equiv \Delta(T)\,, \tag{3.3}$$

where e denotes the energy density. In the context of QCD this quantity is referred to as the trace anomaly, and has been studied with lattice methods. Were it not that chiral fermions (in particular the top quark) are essential for the physics considered, the problem could in principle be studied with full 4-dimensional lattice simulations here as well. In the present paper, we circumvent the problem of chiral fermions by using lattice input only for the Bose-enhanced infrared degrees of freedom, treating fermions within a (resummed) weak-coupling expansion.

Now, because of dimensional reasons, we may rewrite eq. (3.1) as

$$\frac{p(T)}{T^4} \equiv \hat{p}_{\mathrm{R}}\left(\frac{\bar{\mu}}{T}, \frac{\nu^2(\bar{\mu})}{T^2}, g^2(\bar{\mu})\right) - \frac{p_{0\mathrm{R}}}{T^4}\left(\bar{\mu}, \nu^2(\bar{\mu}), g^2(\bar{\mu})\right)\,. \tag{3.4}$$

We note from the Euclidean path integral representation, *viz.*

$$\mathcal{Z} = \int \mathcal{D}[\ldots]\,\exp\Big\{-\int_V \mathrm{d}^{3-2\epsilon}\mathbf{x}\int_0^{1/T}\mathrm{d}\tau\mathcal{L}_{\mathrm{E}}\Big\}\,, \tag{3.5}$$

that the bare pressure obeys (here $\hat{p}_{\mathrm{B}} \equiv p_{\mathrm{B}}/T^4$)

$$\frac{\partial\hat{p}_{\mathrm{B}}}{\partial(\nu^2(\bar{\mu})/T^2)} = \frac{[\mathcal{Z}_m\langle\phi^\dagger\phi\rangle]_{\mathrm{B}}}{T^2}\,, \tag{3.6}$$

where we wrote $\nu_{\mathrm{B}}^2 = \mathcal{Z}_m\,\nu^2(\bar{\mu})$.[3] It is now straightforward to obtain the following relation:

$$T\frac{\mathrm{d}}{\mathrm{d}T}\left\{\frac{p(T)}{T^4}\right\} = -\frac{\partial\hat{p}_{\mathrm{R}}}{\partial\ln(\bar{\mu}/T)} - \frac{2\nu^2(\bar{\mu})\,[\mathcal{Z}_m\langle\phi^\dagger\phi\rangle]_{\mathrm{R}}}{T^4} + \frac{4p_{0\mathrm{R}}}{T^4}\,. \tag{3.7}$$

Here eq. (3.6) has been replaced by its renormalized version.

It can be observed from eq. (3.7) that three ingredients are needed: the determination of explicit logarithms appearing in $\hat{p}_{\mathrm{R}}$ ("breaking of scale invariance by quantum corrections"); the temperature evolution of the Higgs condensate ("explicit breaking of scale invariance"); as well as the vacuum term needed for renormalization. We discuss the first of these in the next section, the condensate in section 5, and the vacuum term in section 6. The results are collected together and evaluated numerically in section 7.

4 Effects from scale violation by quantum corrections

The first ingredient needed in eq. (3.7) are logarithms of $\bar{\mu}/T$ that are induced by loop corrections. There are two ways to extract $\frac{\partial\hat{p}_{\mathrm{R}}}{\partial\ln(\bar{\mu}/T)}$ from ref. [18]: either by reading logarithms from the explicit expressions for the various coefficients given there, or by deducing them from the running of the couplings. Making use of the notation in eq. (2.5), with $\hat{p} \equiv p/T^4$, the part $\hat{p}_{\mathrm{G}}$ contributes at $\mathcal{O}(g^6)$. From $\hat{p}_{\mathrm{E}} + \hat{p}_{\mathrm{M}}$ we need terms up to and including $\mathcal{O}(g^5)$. The expansion reads

$$\begin{aligned}\hat{p}_{\mathrm{E}} + \hat{p}_{\mathrm{M}} = {} & \alpha_{\mathrm{E}1} + g_1^2\alpha_{\mathrm{EB}} + g_2^2\alpha_{\mathrm{EA}} + g_3^2\alpha_{\mathrm{EC}} + \lambda\alpha_{\mathrm{E}\lambda} + h_t^2\alpha_{\mathrm{EY}} + \frac{\nu^2}{T^2}\alpha_{\mathrm{E}\nu} \\ & + \frac{\nu^4}{(4\pi)^2T^4}\left(\frac{1}{\epsilon} + \alpha_{\mathrm{E}\nu\nu}\right) + \frac{1}{12\pi T^3}\left[\left(m_{\mathrm{E}1}^{2\,(0)}\right)^{\frac{3}{2}} + 3\left(m_{\mathrm{E}2}^{2\,(0)}\right)^{\frac{3}{2}} + 8\left(m_{\mathrm{E}3}^{2\,(0)}\right)^{\frac{3}{2}}\right] + \ldots\,,\end{aligned} \tag{4.1}$$

[3] The renormalization factor reads $\mathcal{Z}_m = 1 + \frac{3}{(4\pi)^2\epsilon}\left[2\lambda + h_t^2 - \frac{1}{4}\left(g_1^2 + 3g_2^2\right)\right] + \mathcal{O}(g^4)$ but is not separately needed, because it always appears in the combination $\mathcal{Z}_m\langle\phi^\dagger\phi\rangle$.

where the leading-order Debye masses read ($n_{\mathrm{G}} = 3$ denotes the number of generations)

$$m_{\mathrm{E1}}^{2\,(0)} = \left(\frac{1}{6} + \frac{5n_{\mathrm{G}}}{9}\right) g_1^2 T^2\,, \quad m_{\mathrm{E2}}^{2\,(0)} = \left(\frac{5}{6} + \frac{n_{\mathrm{G}}}{3}\right) g_2^2 T^2\,, \quad m_{\mathrm{E3}}^{2\,(0)} = \left(1 + \frac{n_{\mathrm{G}}}{3}\right) g_3^2 T^2\,. \tag{4.2}$$

All coefficients in eq. (4.1) apart from $\alpha_{\mathrm{E}\nu\nu}$ are scale independent; its value differs from that in ref. [18] because of our different renormalization condition:

$$\alpha_{\mathrm{E}\nu\nu} = d_{\mathrm{F}} n_{\mathrm{S}} \left(\ln \frac{\bar{\mu}}{4\pi T} + \gamma_{\mathrm{E}}\right), \tag{4.3}$$

where $d_{\mathrm{F}}, n_{\mathrm{S}}$ are specified in eq. (B.1). Given that the pressure as a whole is scale independent, running from the couplings must cancel against explicit logarithms; therefore,

$$\begin{aligned}\frac{\partial[\hat{p}_{\mathrm{E}} + \hat{p}_{\mathrm{M}}]_{\mathrm{R}}}{\partial \ln(\bar{\mu}/T)} = {} & -\alpha_{\mathrm{EB}}\,\bar{\mu}\frac{\mathrm{d}g_1^2}{\mathrm{d}\bar{\mu}} - \alpha_{\mathrm{EA}}\,\bar{\mu}\frac{\mathrm{d}g_2^2}{\mathrm{d}\bar{\mu}} - \alpha_{\mathrm{EC}}\,\bar{\mu}\frac{\mathrm{d}g_3^2}{\mathrm{d}\bar{\mu}} - \alpha_{\mathrm{E}\lambda}\,\bar{\mu}\frac{\mathrm{d}\lambda}{\mathrm{d}\bar{\mu}} - \alpha_{\mathrm{EY}}\,\bar{\mu}\frac{\mathrm{d}h_t^2}{\mathrm{d}\bar{\mu}} - \frac{\alpha_{\mathrm{E}\nu}}{T^2}\,\bar{\mu}\frac{\mathrm{d}\nu^2}{\mathrm{d}\bar{\mu}} \\ & + \frac{\nu^4}{(4\pi)^2 T^4}\,\bar{\mu}\frac{\mathrm{d}\alpha_{\mathrm{E}\nu\nu}}{\mathrm{d}\bar{\mu}} - \sum_{i=1}^{3} \frac{d_i m_{\mathrm{E}i}^{(0)}}{8\pi T^3}\,\bar{\mu}\frac{\mathrm{d}m_{\mathrm{E}i}^{2\,(0)}}{\mathrm{d}\bar{\mu}} + \mathcal{O}(g^6)\,,\end{aligned} \tag{4.4}$$

where $d_1 \equiv 1$, $d_2 \equiv 3$, and $d_3 \equiv 8$. The runnings can be read from eqs. (7)–(12) of ref. [18]. Putting together, we obtain

$$-\frac{\partial[\hat{p}_{\mathrm{E}} + \hat{p}_{\mathrm{M}}]_{\mathrm{R}}}{\partial \ln(\bar{\mu}/T)} = \Delta_1(T)\,, \tag{4.5}$$

$$\begin{aligned}\Delta_1(T) \equiv {} & \frac{1}{(4\pi)^2}\left\{\frac{198 + 141n_{\mathrm{G}} - 20n_{\mathrm{G}}^2}{54} g_3^4 + \frac{266 + 163n_{\mathrm{G}} - 40n_{\mathrm{G}}^2}{288} g_2^4\right. \\ & - \frac{144 + 375n_{\mathrm{G}} + 1000n_{\mathrm{G}}^2}{7776} g_1^4 - \frac{g_2^2 g_1^2}{32} - h_t^2\left(\frac{7h_t^2}{32} - \frac{5g_3^2}{6} - \frac{15g_2^2}{64} - \frac{85g_1^2}{576}\right) \\ & \left. - \lambda\left(\lambda + \frac{h_t^2}{2} - \frac{g_1^2 + 3g_2^2}{8}\right) + \frac{\nu^2}{T^2}\left(h_t^2 + 2\lambda - \frac{g_1^2 + 3g_2^2}{4}\right) - \frac{2\nu^4}{T^4}\right\} \\ & - \frac{1}{(4\pi)^3}\left\{32 g_3^5 \left(1 + \frac{n_{\mathrm{G}}}{3}\right)^{\frac{3}{2}} \left(\frac{11}{4} - \frac{n_{\mathrm{G}}}{3}\right) + 12 g_2^5 \left(\frac{5}{6} + \frac{n_{\mathrm{G}}}{3}\right)^{\frac{3}{2}} \left(\frac{43}{24} - \frac{n_{\mathrm{G}}}{3}\right)\right. \\ & \left. - 4 g_1^5 \left(\frac{1}{6} + \frac{5n_{\mathrm{G}}}{9}\right)^{\frac{3}{2}} \left(\frac{1}{24} + \frac{5n_{\mathrm{G}}}{9}\right)\right\} + \mathcal{O}(g^6)\,.\end{aligned} \tag{4.6}$$

This expression is renormalization group (RG) invariant up to $\mathcal{O}(g^6)$. The numerically largest corrections originate from terms involving the strong gauge coupling g_3^2.

5 Effects from the Higgs condensate

5.1 Outline

The Higgs condensate can be obtained from eq. (3.6). For a non-perturbative evaluation, we make use of the lattice simulations in refs. [6, 21]. This means that we split the pressure into contributions from various momentum scales like in eq. (2.5):

$$\mathcal{Z}_m \langle \phi^\dagger \phi \rangle = \frac{\partial p_{\mathrm{E}}}{\partial \nu^2} + \frac{\partial p_{\mathrm{M}}}{\partial \nu^2} + \frac{\partial p_{\mathrm{G}}}{\partial \nu^2}\,. \tag{5.1}$$

Given that $\mathcal{Z}_m \langle \phi^\dagger \phi \rangle$ is multiplied by ν^2 in eq. (3.7) and that we assume $\nu^2 \sim g^2 T^2$, we only need to determine $\mathcal{Z}_m \langle \phi^\dagger \phi \rangle$ to $\mathcal{O}(g^3)$. That said, it turns out that computations going beyond those in refs. [18, 19] are needed.

JCAP07(2015)035

5.2 Perturbative contributions

The first term of eq. (5.1), the contribution from the "hard" scales $k \sim \pi T$, can be directly extracted from the results of ref. [18]:

$$\frac{\partial p_{\rm E}}{\partial \nu^2} = T^2 \biggl\{ \alpha_{{\rm E}\nu} + \frac{g_1^2 \alpha_{{\rm EB}\nu} + g_2^2 \alpha_{{\rm EA}\nu} + \lambda \alpha_{{\rm E}\lambda\nu} + h_t^2 \alpha_{{\rm EY}\nu}}{(4\pi)^2} \biggr\} + \frac{2\nu^2}{(4\pi)^2} \biggl(\frac{1}{\epsilon} + \alpha_{{\rm E}\nu\nu} \biggr) + \mathcal{O}(g^4) \,. \tag{5.2}$$

Inserting coefficients from ref. [18] and from eq. (4.3), this contains $1/\epsilon$-divergences in the terms proportional to g_1^2, g_2^2 and ν^2:

$$\begin{aligned} \frac{\partial p_{\rm E}}{\partial \nu^2} = \frac{T^2}{6} \biggl\{ 1 - \frac{1}{(4\pi)^2} \biggl[\frac{3}{2} (g_1^2 + 3 g_2^2) \biggl(\frac{1}{\epsilon} + 3 \ln \frac{\bar{\mu}}{4\pi T} + \gamma_{\rm E} + \frac{5}{3} + \frac{2\zeta'(-1)}{\zeta(-1)} \biggr) \\ + 6 h_t^2 \biggl(\ln \frac{\bar{\mu}}{8\pi T} + \gamma_{\rm E} \biggr) + 12 \lambda \biggl(\ln \frac{\bar{\mu}}{4\pi T} + \gamma_{\rm E} \biggr) \biggr] \biggr\} \\ + \frac{4\nu^2}{(4\pi)^2} \biggl(\frac{1}{2\epsilon} + \ln \frac{\bar{\mu}}{4\pi T} + \gamma_{\rm E} \biggr) + \mathcal{O}(g^4) \,. \end{aligned} \tag{5.3}$$

The second term of eq. (5.1), the contribution from the "soft" scales $k \sim gT$, originates at $\mathcal{O}(g^3)$ from the dependence of the effective mass parameters on ν^2:

$$\frac{\partial p_{\rm M}}{\partial \nu^2} = \sum_{i=1}^{2} \frac{\partial m_{{\rm E}i}^2}{\partial \nu^2} \frac{\partial p_{\rm M}}{\partial m_{{\rm E}i}^2} + \frac{\partial m_3^2}{\partial \nu^2} \frac{\partial p_{\rm M}}{\partial m_3^2} + \mathcal{O}(g^6) \,. \tag{5.4}$$

The first two terms give contributions that can be extracted from [19]: the Debye mass parameters depend on ν^2 as

$$m_{\rm E1}^2 = g_1^2 \biggl[T^2 \beta'_{\rm E1} - \frac{\nu^2}{(4\pi)^2} \beta'_{{\rm E}\nu} \biggr] + \ldots \,, \quad m_{\rm E2}^2 = g_2^2 \biggl[T^2 \beta_{\rm E1} - \frac{\nu^2}{(4\pi)^2} \beta_{{\rm E}\nu} \biggr] + \ldots \,, \tag{5.5}$$

where $\beta'_{\rm E1}$ and $\beta_{\rm E1}$ are as in eq. (4.2). Differentiating the term on the second line of eq. (4.1) and inserting the values of the coefficients from ref. [19] yields

$$\sum_{i=1}^{2} \frac{\partial m_{{\rm E}i}^2}{\partial \nu^2} \frac{\partial p_{\rm M}}{\partial m_{{\rm E}i}^2} = - \frac{T^2}{(4\pi)^3} \biggl[3 g_2^3 \biggl(\frac{5}{6} + \frac{n_{\rm G}}{3} \biggr)^{\frac{1}{2}} + g_1^3 \biggl(\frac{1}{6} + \frac{5 n_{\rm G}}{9} \biggr)^{\frac{1}{2}} \biggr] + \mathcal{O}(g^4) \,. \tag{5.6}$$

The last term of eq. (5.4) also contributes, but this contribution cannot be extracted from ref. [19]. The reason is that if we consider $p_{\rm M}$ *without* a derivative, then contributions involving m_3^2 are of $\mathcal{O}(g^6)$ for $|m_3^2| \lesssim g^3 T^2/\pi$. However, the derivative of m_3^2 is larger than m_3^2 itself: $\nu^2 \partial m_3^2/\partial \nu^2 \sim \nu^2 \sim g^2 T^2$. Therefore terms that are of higher order in $p_{\rm M}$ do contribute to the trace anomaly.

The computation of $\partial p_{\rm M}/\partial m_3^2$ is simplified by the fact that since the softest physics is captured by a study of $p_{\rm G}$, the Higgs and gauge fields can be treated as massless in the computation of the matching coefficient $p_{\rm M}$. Then most diagrams, in particular all diagrams which do not contain at least one adjoint scalar propagator, vanish in dimensional regularization. The leading non-zero contributions, which are the only terms needed at $\mathcal{O}(g^3)$, are those given in figure 1. Reducing the diagrams to master integrals and evaluating them with standard techniques (cf. e.g. ref. [22]), we obtain

$$\frac{\partial m_3^2}{\partial \nu^2} \frac{\partial p_{\rm M}}{\partial m_3^2} = - \frac{T^3}{16(4\pi)^3} \biggl[\frac{g_2^4}{m_{\rm E2}} \biggl(- \frac{2}{\epsilon} - 12 \ln \frac{\bar{\mu}}{2 m_{\rm E2}} + \frac{35}{3} \biggr) + \frac{g_1^4}{m_{\rm E1}} + \frac{12 g_1^2 g_2^2}{m_{\rm E1} + m_{\rm E2}} \biggr] \,. \tag{5.7}$$

JCAP07(2015)035

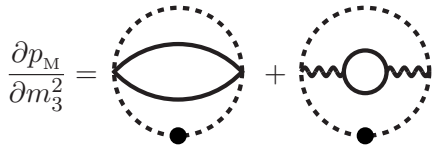

Figure 1. Processes representing $\partial p_{\rm M}/\partial m_3^2$. The filled blob is $m_3^2\,\phi^\dagger\phi$; dashed lines are scalar propagators; solid lines are adjoint scalar propagators; and wiggly lines are gauge fields. All 1-loop and 2-loop diagrams and all other 3-loop diagrams vanish in dimensional regularization.

5.3 Non-perturbative contribution

The third term of eq. (5.1), the contribution from the "ultrasoft" scales $k \sim g^2T/\pi$, can be expressed as

$$\frac{\partial p_{\rm G}}{\partial \nu^2} = \frac{\partial \bar{m}_3^2}{\partial \nu^2}\frac{\partial p_{\rm G}}{\partial \bar{m}_3^2} + \mathcal{O}(g^8)\,, \tag{5.8}$$

where $\bar{m}_3^2$ is the Higgs mass parameter within MSM and the error comes from partial derivatives with respect to the other effective couplings of MSM. The dependence of $\bar{m}_3^2$ on ν^2 is known up to $\mathcal{O}(g^2)$ [13], with the leading term reading $\partial\bar{m}_3^2/\partial\nu^2 = -1$. The condensate can be expressed in dimensional regularization as

$$-\frac{\partial p_{\rm G}}{\partial \bar{m}_3^2} = \frac{(g_{\rm M1}^2 + 3g_{\rm M2}^2)T}{(4\pi)^2}\left(\frac{1}{4\epsilon} + \ln\frac{\bar{\mu}}{g_{\rm M2}^2}\right) + \langle\phi^\dagger\phi\rangle_{\rm 3d}(g_{\rm M2}^2)\,, \tag{5.9}$$

where the argument of $\langle\phi^\dagger\phi\rangle_{\rm 3d}$ indicates the renormalization scale used within MSM. As discussed below eq. (2.3) the condensate is parametrically $\lesssim gT^2$ in our power counting, and therefore we keep the correction of $\mathcal{O}(g^2)$ in the coefficient of $\langle\phi^\dagger\phi\rangle_{\rm 3d}$, even though we do not keep it in the ultraviolet part where it is unambiguously of $\mathcal{O}(g^4)$. For future reference we express the ultraviolet part in terms of the couplings of the full theory, by inserting[4]

$$g_{\rm M2}^2 = g_2^2T\left[1 - \frac{g_2^2T}{24\pi m_{\rm E2}}\left(1 + 2\epsilon\ln\frac{\bar{\mu}}{2m_{\rm E2}}\right)\right] + \mathcal{O}(g^4)\,, \tag{5.12}$$

$$g_{\rm M1}^2 = g_1^2T + \mathcal{O}(g^4)\,. \tag{5.13}$$

Thereby the ultrasoft contribution from $k \sim g^2T/\pi$ becomes

$$\begin{aligned}\frac{\partial\bar{m}_3^2}{\partial\nu^2}\frac{\partial p_{\rm G}}{\partial\bar{m}_3^2} = {}& \left\{1 + \frac{3}{2(4\pi)^2}\left[(g_1^2 + 3g_2^2 - 8\lambda)\ln\left(\frac{\bar{\mu}e^{\gamma_{\rm E}}}{4\pi T}\right) - 4h_t^2\ln\left(\frac{\bar{\mu}e^{\gamma_{\rm E}}}{\pi T}\right)\right]\right\}\langle\phi^\dagger\phi\rangle_{\rm 3d}(g_{\rm M2}^2) \\ & + \frac{(g_1^2 + 3g_2^2)T^2}{(4\pi)^2}\left(\frac{1}{4\epsilon} + \ln\frac{\bar{\mu}}{g_{\rm M2}^2}\right) \\ & - \frac{g_2^4T^3}{2(4\pi)^3 m_{\rm E2}}\left(\frac{1}{4\epsilon} + \ln\frac{\bar{\mu}}{g_{\rm M2}^2} + \frac{1}{2}\ln\frac{\bar{\mu}}{2m_{\rm E2}}\right) + \mathcal{O}(g^4)\,.\end{aligned} \tag{5.14}$$

[4]For $g_{\rm M2}^2$ corrections are known up to 2-loop order [23]. The other parameters of MSM read:

$$\lambda_{\rm M} = \lambda_{\rm E} - \frac{1}{8\pi}\left[\frac{3g_{\rm E2}^4}{16m_{\rm E2}} + \frac{g_{\rm E1}^2g_{\rm E2}^2}{4(m_{\rm E1}+m_{\rm E2})} + \frac{g_{\rm E1}^4}{16m_{\rm E1}}\right], \tag{5.10}$$

$$\begin{aligned}\bar{m}_{\rm 3B}^2 = {}& m_{\rm 3B}^2 - \frac{1}{16\pi}\left(g_{\rm E1}^2m_{\rm E1} + 3g_{\rm E2}^2m_{\rm E2}\right) + \frac{1}{8(4\pi)^2}\left[15g_{\rm E2}^4\left(\frac{1}{4\epsilon} + \ln\frac{\bar{\mu}}{2m_{\rm E2}} + \frac{3}{10}\right)\right. \\ & \left. - 6g_{\rm E1}^2g_{\rm E2}^2\left(\frac{1}{4\epsilon} + \ln\frac{\bar{\mu}}{m_{\rm E1}+m_{\rm E2}} + \frac{1}{2}\right) - g_{\rm E1}^4\left(\frac{1}{4\epsilon} + \ln\frac{\bar{\mu}}{2m_{\rm E1}} + \frac{1}{2}\right)\right].\end{aligned} \tag{5.11}$$

These are needed if one wants to deduce eq. (5.7) directly from eq. (35) of ref. [18] by taking $m_{\rm E1}, m_{\rm E2} \gg m_3$.

JCAP07(2015)035

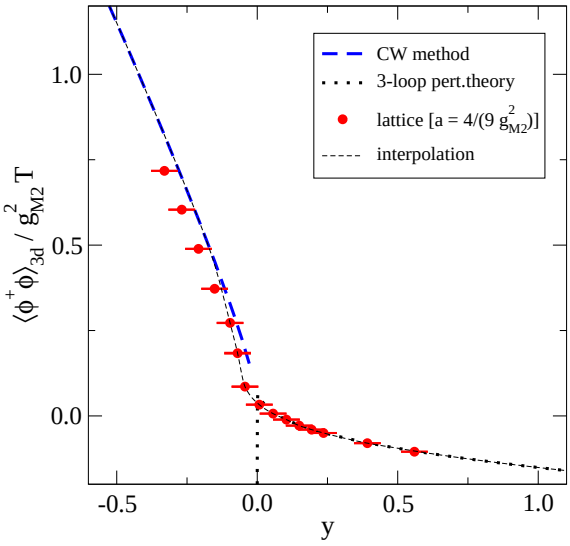

Figure 2. The $\overline{\rm MS}$ renormalized 3d condensate (cf. eq. (5.9)) according to lattice simulations [6] and perturbation theory (cf. appendix A), as a function of y from eq. (A.2). The lattice data corresponds to a fixed lattice spacing a, which induces errors particularly at low temperatures [21]. For the results of section 7 the phenomenological interpolation indicated with the thin dashed line is employed.

The condensate $\langle\phi^\dagger\phi\rangle_{\rm 3d}(g^2_{\rm M2})$ can be measured non-perturbatively by subtracting proper counterterms [24] from lattice measurements extrapolated to the infinite-volume limit, and extrapolating subsequently to the continuum limit. A continuum extrapolation has only been carried out at an unphysically small Higgs mass [21] but cutoff effects have been seen to be modest, as long as we are not in the broken phase. Therefore we make use of lattice results at the physical Higgs mass [6] only for $-0.1 \lesssim y \lesssim 0.2$ in terms of the parameters in eq. (A.2). In order to extrapolate to higher or lower temperatures, perturbative expressions are employed; their values are discussed in appendix A. The procedure is illustrated in figure 2.

5.4 Combined expression

Summing together the contributions from eqs. (5.3), (5.6), (5.7) and (5.14), most of the $1/\epsilon$-divergences cancel, and we get

$$-\frac{2\nu^2\mathcal{Z}_m\langle\phi^\dagger\phi\rangle}{T^4} = \Delta_2(T;\bar\mu) - \frac{4\nu^4}{(4\pi)^2T^4\epsilon} + \mathcal{O}(g^6)\,, \tag{5.15}$$

where the finite part reads

$$\begin{aligned}
\Delta_2(T;\bar\mu) \equiv {} & -\frac{2\nu^2}{T^4}\left\{1+\frac{3}{2(4\pi)^2}\left[(g_1^2+3g_2^2-8\lambda)\ln\left(\frac{\bar\mu e^{\gamma_{\rm E}}}{4\pi T}\right)-4h_t^2\ln\left(\frac{\bar\mu e^{\gamma_{\rm E}}}{\pi T}\right)\right]\right\}\langle\phi^\dagger\phi\rangle_{\rm 3d}(g^2_{\rm M2}) \\
& -\frac{\nu^2}{3T^2}\left\{1-\frac{3}{2(4\pi)^2}\left[(g_1^2+3g_2^2)\left(4\ln\frac{g^2_{\rm M2}}{\bar\mu}+3\ln\frac{\bar\mu}{4\pi T}+\gamma_{\rm E}+\frac{5}{3}+\frac{2\zeta'(-1)}{\zeta(-1)}\right)\right.\right. \\
& \left.\left.+4h_t^2\ln\left(\frac{\bar\mu e^{\gamma_{\rm E}}}{8\pi T}\right)+8\lambda\ln\left(\frac{\bar\mu e^{\gamma_{\rm E}}}{4\pi T}\right)\right]\right\} \\
& +\frac{2\nu^2}{(4\pi)^3T^2}\left[\frac{g_1^2m_{\rm E1}+3g_2^2m_{\rm E2}}{T}+\frac{g_1^4T}{16m_{\rm E1}}+\frac{3g_1^2g_2^2T}{4(m_{\rm E1}+m_{\rm E2})}+\frac{g_2^4T}{2m_{\rm E2}}\left(\frac{35}{24}+\ln\frac{2m_{\rm E2}}{g^2_{\rm M2}}\right)\right] \\
& -\frac{8\nu^4}{(4\pi)^2T^4}\ln\left(\frac{\bar\mu e^{\gamma_{\rm E}}}{4\pi T}\right)\,.
\end{aligned} \tag{5.16}$$

JCAP07(2015)035

Apart from the last term the result is $\bar{\mu}$-independent up to $\mathcal{O}(g^6)$. This $\bar{\mu}$-dependence as well as the divergence in eq. (5.15) cancel against terms from the vacuum subtraction, cf. section 6.

6 Vacuum subtraction and renormalization

Suppose that we compute the bare vacuum pressure, $p_{0\mathrm{B}}$, in a perturbative loop expansion: $p_{0\mathrm{B}} = \sum_\ell p_{0\mathrm{B}}^{(\ell)}$. In a gauge-fixed computation, the result is a function of the Higgs expectation value, which can likewise be determined order by order: $v = \sum_\ell v^{(\ell)}$. Even though v is gauge-dependent, $p_{0\mathrm{B}}$ is gauge-independent order by order in perturbation theory. Inserting v into $p_{0\mathrm{B}}$, we can re-expand the result as

$$p_{0\mathrm{B}} = p_{0\mathrm{B}}^{(0)}\left(v^{(0)} + v^{(1)} + \dots\right) + p_{0\mathrm{B}}^{(1)}\left(v^{(0)} + \dots\right) + \dots = p_{0\mathrm{B}}^{(0)}\left(v^{(0)}\right) + p_{0\mathrm{B}}^{(1)}\left(v^{(0)}\right) + \dots\,, \tag{6.1}$$

where we made use of $p_{0\mathrm{B}}^{(0)} = p_{0\mathrm{R}}^{(0)}$ and $[p_{0\mathrm{R}}^{(0)}]'(v^{(0)}) = 0$. The terms not shown are of $\mathcal{O}(g^6)$ in our power counting. Therefore, it is sufficient for our purposes to compute $p_{0\mathrm{B}}$ up to 1-loop level and insert the tree-level Higgs vacuum expectation value $v^2 = \nu^2/\lambda$ into the expression.

Dropping the superscripts, we get

$$\begin{aligned} p_{0\mathrm{B}} = \Bigg\{ & \frac{1}{2}(\nu^2 + \delta\nu^2)v^2 - \frac{1}{4}(\lambda + \delta\lambda)v^4 \\ & + \frac{3m_W^4}{32\pi^2}\left(\frac{1}{\epsilon} + \ln\frac{\bar{\mu}^2}{m_W^2} + \frac{5}{6}\right) + \frac{3m_Z^4}{64\pi^2}\left(\frac{1}{\epsilon} + \ln\frac{\bar{\mu}^2}{m_Z^2} + \frac{5}{6}\right) \\ & + \frac{m_H^4}{64\pi^2}\left(\frac{1}{\epsilon} + \ln\frac{\bar{\mu}^2}{m_H^2} + \frac{3}{2}\right) - \frac{3m_t^4}{16\pi^2}\left(\frac{1}{\epsilon} + \ln\frac{\bar{\mu}^2}{m_t^2} + \frac{3}{2}\right)\Bigg\}_{v^2=\nu^2/\lambda} + \mathcal{O}(g^6)\,. \end{aligned} \tag{6.2}$$

The counterterms read

$$\delta\nu^2 = \frac{3\nu^2}{(4\pi)^2\epsilon}\left[-\frac{g_1^2 + 3g_2^2}{4} + h_t^2 + 2\lambda\right], \tag{6.3}$$

$$\delta\lambda = \frac{3}{(4\pi)^2\epsilon}\left[\frac{g_1^4 + 2g_1^2g_2^2 + 3g_2^4}{16} - h_t^2\left(h_t^2 - 2\lambda\right) + \lambda\left(4\lambda - \frac{g_1^2 + 3g_2^2}{2}\right)\right], \tag{6.4}$$

whereas at the minimum the masses take the values

$$m_W^2 = \frac{g_2^2\nu^2}{4\lambda}\,, \quad m_Z^2 = \frac{(g_1^2 + g_2^2)\nu^2}{4\lambda}\,, \quad m_H^2 = 2\nu^2\,, \quad m_t^2 = \frac{h_t^2\nu^2}{2\lambda}\,. \tag{6.5}$$

Most divergences cancel, and the vacuum result becomes

$$\frac{4p_{0\mathrm{B}}}{T^4} = \Delta_3(T;\bar{\mu}) + \frac{4\nu^4}{(4\pi)^2T^4\epsilon}\,, \tag{6.6}$$

where

$$\begin{aligned} \Delta_3(T;\bar{\mu}) \equiv & \frac{\nu^4}{\lambda T^4} + \frac{4\nu^4}{(4\pi)^2T^4}\left[\ln\frac{\bar{\mu}^2}{\nu^2} + \frac{3}{2}\right] \\ & + \frac{3\nu^4}{\lambda^2(16\pi)^2T^4}\left\{2g_2^4\left[\ln\frac{4\lambda\bar{\mu}^2}{g_2^2\nu^2} + \frac{5}{6}\right] + (g_1^2 + g_2^2)^2\left[\ln\frac{4\lambda\bar{\mu}^2}{(g_1^2 + g_2^2)\nu^2} + \frac{5}{6}\right]\right\} \\ & - \frac{3\nu^4h_t^4}{\lambda^2(4\pi)^2T^4}\left[\ln\frac{2\lambda\bar{\mu}^2}{h_t^2\nu^2} + \frac{3}{2}\right] + \mathcal{O}(g^6)\,. \end{aligned} \tag{6.7}$$

JCAP07(2015)035

In practice, it is not useful to evaluate eq. (6.7) directly, because our renormalization scale will be $\bar{\mu} \sim \pi T$, which would introduce large logarithms if inserted into eq. (6.7). Rather, all vacuum parameters are first evaluated at a scale $\bar{\mu}_0 \equiv m_Z$, and then evolved from $\bar{\mu}_0$ to the thermal scale through RG equations. As an illustration, the 1-loop RG equations for the two dimensionful parameters appearing in our analysis read

$$\bar{\mu}\frac{\mathrm{d}\nu^2}{\mathrm{d}\bar{\mu}} = \frac{3\nu^2}{8\pi^2}\left(-\frac{g_1^2+3g_2^2}{4} + h_t^2 + 2\lambda\right), \tag{6.8}$$

$$\bar{\mu}\frac{\mathrm{d}p_{0\mathrm{R}}}{\mathrm{d}\bar{\mu}} = \frac{\nu^4}{8\pi^2}, \tag{6.9}$$

from where we get $\Delta_3(T;\bar{\mu}) = 4p_{0\mathrm{R}}/T^4$. At the scale $\bar{\mu} = \bar{\mu}_0$, the running couplings are expressed in terms of physical parameters through 1-loop relations specified e.g. in ref. [13]. (For many parameters a higher loop order could be extracted from more recent literature, but such corrections are smaller than thermal uncertainties, so for the sake of simplicity and reproducibility we make use of explicit 1-loop expressions.)

7 Phenomenological results

Summing together the terms from eqs. (4.6), (5.15), (6.6) as dictated by eq. (3.7), all $1/\epsilon$-divergences cancel, and we obtain

$$T\frac{\mathrm{d}}{\mathrm{d}T}\left\{\frac{p(T)}{T^4}\right\} = \Delta_1(T) + \Delta_2(T;\bar{\mu}) + \Delta_3(T;\bar{\mu}) + \mathcal{O}(g^6)\,. \tag{7.1}$$

Because of a cancellation between Δ_2 and Δ_3 the result is formally independent of the renormalization scale $\bar{\mu}$, even though in practice a residual $\bar{\mu}$-dependence is left over, as a reflection of unknown higher order corrections. We write $\bar{\mu} = \alpha\pi T$, and vary α in the range $\alpha \in (0.5\ldots2.0)$ in order to get one impression on the corresponding uncertainty.

The result of eq. (7.1) is accurate up to and including the order $\mathcal{O}(g^5)$. It is well known from studies of the pressure of QCD, however, that certain odd orders show anomalously poor convergence. In particular, whereas the $\mathcal{O}(g^2)$ correction to the pressure provides for a reasonable approximation, the $\mathcal{O}(g^3)$ correction is far off. For Δ, the order $\mathcal{O}(g^4)$ is related to the $\mathcal{O}(g^2)$ correction to the pressure, and the order $\mathcal{O}(g^5)$ to the $\mathcal{O}(g^3)$ correction (cf. section 4). For this reason, the numerically most accurate estimate for Δ can probably be obtained by restricting to $\mathcal{O}(g^4)$. A result corresponding to this accuracy is shown for the observable of eq. (7.1) in figure 3. (For the pressure we display also the $\mathcal{O}(g^5)$ result in figure 4(left).)

In order to obtain other thermodynamic functions, the boundary value needed for eq. (3.2) should be fixed. We do this on the low-temperature side, making use of the results of ref. [25][5] and thereby setting $p(T_0)/T_0^4 \simeq 10.91$ at $T_0 = 100\,\mathrm{GeV}$. On the high-temperature side, we expect to match to the results of ref. [18], after changing the overall renormalization condition to our eq. (2.6) and by making the changes listed in appendix B. Like for Δ, we make use of the result of $\mathcal{O}(g^4)$, with the negative $\mathcal{O}(g^5)$ QCD contribution expected to lead to an underestimate [26, 27]. (We have also experimented with an approximate $\mathcal{O}(g^6)$ QCD contribution as estimated in ref. [25], finding a result which is in between the $\mathcal{O}(g^4)$ and $\mathcal{O}(g^5)$ ones, confirming that the $\mathcal{O}(g^5)$ result is most likely on the low side.)

[5] Tabulated results can be downloaded from www.laine.itp.unibe.ch/eos06/.

JCAP07(2015)035

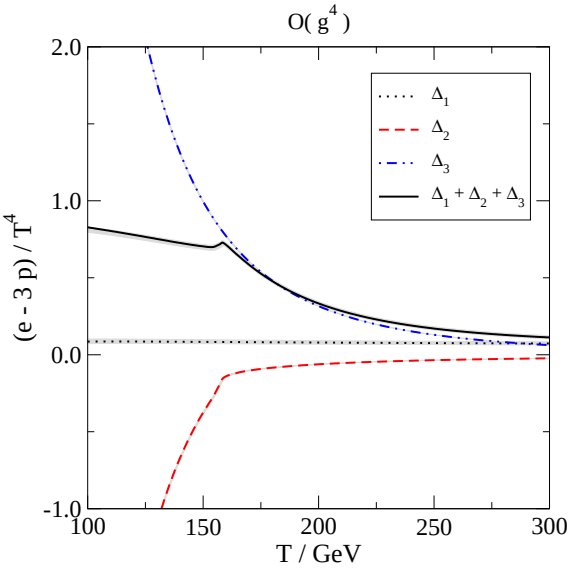

Figure 3. The trace "anomaly" from eq. (7.1). The grey band reflects variations of the renormalization scale in the range $\bar{\mu} = (0.5 \ldots 2.0)\pi T$. Contributions of $\mathcal{O}(\nu^4/T^4)$ are seen to cancel at low temperatures.

After choosing an initial condition, other thermodynamic functions are obtained as follows: the pressure p/T^4 from eq. (3.2); the energy density from $e/T^4 = \Delta + 3p/T^4$; the entropy density $s = p'$ from $s/T^3 = \Delta + 4p/T^4$; the heat capacity $c = e'$ from $c/T^3 = T\Delta' + 7\Delta + 12p/T^4$; the equation-of-state parameter from $w = p/e = 1/(3 + \Delta T^4/p)$; and the speed of sound squared from $c_s^2 = p'/e' = s/c$. Some of these functions are conveniently parametrized through

$$g_{\rm eff}(T) \equiv \frac{e(T)}{\left[\frac{\pi^2 T^4}{30}\right]}\,, \quad h_{\rm eff}(T) \equiv \frac{s(T)}{\left[\frac{2\pi^2 T^3}{45}\right]}\,, \quad i_{\rm eff}(T) \equiv \frac{c(T)}{\left[\frac{2\pi^2 T^3}{15}\right]}\,. \tag{7.2}$$

Results for all of these functions are shown in figure 4. (The heat capacity and the speed of sound squared are the most "difficult" quantities, because they require taking a numerical temperature derivative from Δ.)

It may be wondered why our new results do not match exactly the previous ones for high temperatures [18], even though both have been computed up to the same order in g. The main reason is that they involve different sets of higher-order corrections. In particular, eq. (7.1) has been evaluated "strictly" to $\mathcal{O}(g^4)$ or $\mathcal{O}(g^5)$, because this has led to fairly simple expressions. In contrast, the high-temperature result is more cumbersome, including more terms (with non-zero corrections of $\mathcal{O}(1)$, $\mathcal{O}(g^2)$, $\mathcal{O}(g^3)$) and complicated "soft" contributions, because the thermal mass parameters associated with the Higgs and gauge fields are of the same order. For evaluating such contributions the experience from QCD suggests that it is not worth re-expanding them in terms of the original couplings but rather to evaluate $p_{\rm M}$ "as is". We have followed separate procedures for the two regimes, because their difference permits for us to get another impression on the magnitude of unknown higher-order corrections.

Among the various types of error estimates that we have made, that based on scale variations is clearly a lower bound, because it only probes the magnitude of special types of corrections. The error estimate originating from the mismatches of various computations should in principle be a more reliable one, because all types of corrections are included;

JCAP07(2015)035

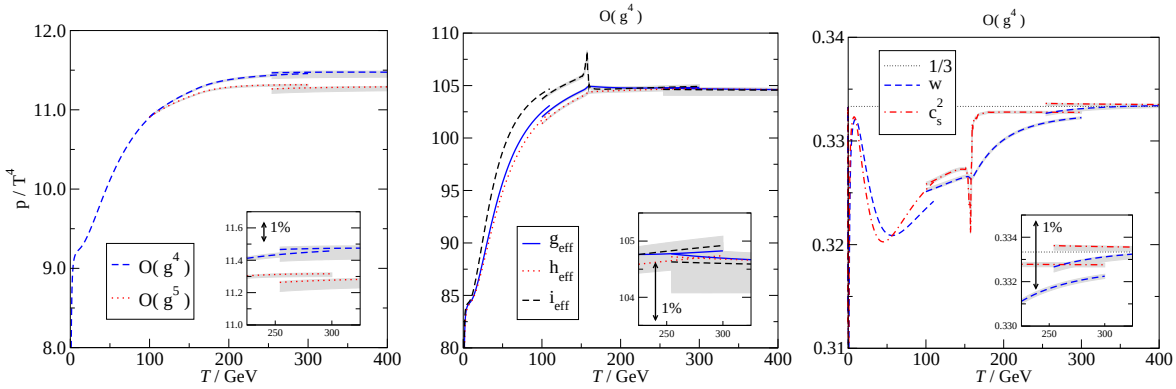

Figure 4. Left: the Standard Model pressure. Middle: $g_{\rm eff}, h_{\rm eff}, i_{\rm eff}$ as defined in eq. (7.2). The heat capacity (parametrized by $i_{\rm eff}$) shows a narrow peak as is characteristic of a rapid crossover. Right: the equation-of-state parameter w and the speed of sound squared c_s^2. The grey bands reflect variations of the renormalization scale in the range $\bar{\mu} = (0.5 \ldots 2.0)\pi T$. The low and high-$T$ results correspond to ref. [25] ($T \lesssim 110\,$GeV) and ref. [18] ($T \gtrsim 250\,$GeV). The close-ups illustrate our estimates of theoretical uncertainties on the high-T side.

nevertheless it should still be treated as a lower bound. In practice, depending on the observable, one of the two gives a more conservative error estimate. In figure 4 both estimates are shown; consequently we expect the theoretical uncertainty of our analysis to be on the percent level. Ultimately, the true accuracy can only be judged by carrying out a non-perturbative analysis of the observables that we have considered.

With the help of the functions in eq. (7.2), the relationship of time and temperature in the Early Universe (assuming a flat geometry) can be expressed as

$$\frac{3}{2}\sqrt{\frac{5}{\pi^3}}\frac{m_{\rm Pl}}{T^3}\frac{{\rm d}T}{{\rm d}t} = -\frac{\sqrt{g_{\rm eff}(T)}h_{\rm eff}(T)}{i_{\rm eff}(T)}\,. \tag{7.3}$$

It is seen that a peak in heat capacity (i.e. $i_{\rm eff}$), visible in figure 4(middle), leads to a short period of slower temperature change [28], and correspondingly a mildly increased abundance of produced particles if a particle production process is under way, or a reduced density of weakly interacting relics disappearing through a co-annihilation process.

8 Conclusions

Drawing on existing multiloop computations [18] and lattice simulations within a dimensionally reduced effective theory [6], and complementing these through new 1-loop, 2-loop and 3-loop computations needed for determining the "trace anomaly" of the electroweak theory, we have estimated the basic thermodynamic functions that play a role for Standard Model thermodynamics at temperatures between 100 GeV and 300 GeV (cf. figure 4). These results can be matched, for most observables with modest ($\sim 1\%$) discrepancies, to perturbative computations at low [25] or high [18] temperatures.

One finding of our study is that despite the high temperatures considered, radiative corrections are larger than might naively be anticipated. Larger corrections also imply that uncertainties are less well under control. On the low-temperature side, we believe that the results of ref. [25] do contain uncertainties because the analysis of the electroweak sector was based on a low loop order and because QCD corrections, whose convergence is slow at

JCAP07(2015)035

finite temperatures, are substantial. On the high-temperature side, the QCD corrections continue to be an issue (cf. figure 4(left)). As an example of the physical significance of these uncertainties, it may be noted from figure 4 that the effective numbers of degrees of freedom remain below the canonical value 106.75 in the whole temperature range considered, and even decrease modestly as the temperature increases above 300 GeV. Even though there could be valid physics reasons for the decrease (such as that the effective Higgs mass parameter is very small across the crossover but then increases again), a similar tendency also originates from the $\mathcal{O}(g^4)$ QCD contribution and is then an artifact of the truncation. (The $\mathcal{O}(g^5)$ correction decreases the effective numbers of degrees of freedom further but turns the results into slowly increasing functions). Another peculiar feature of the $\mathcal{O}(g^4)$ result is that the speed of sound squared c_s^2 is $\sim 0.1\%$ *above* 1/3 at $T > 300\,\mathrm{GeV}$, however this is again reversed by the $\mathcal{O}(g^5)$ correction. In general, the estimated theoretical uncertainty of our results is on the percent level, and no conclusions should be drawn from features finer than this.

In comparison with ref. [25], we find results for the effective numbers of degrees of freedom that are about 1% lower at $T > 300\,\mathrm{GeV}$. The reason is mostly due to negative electroweak radiative corrections proportional to g_2^2 and h_t^2, which were omitted in ref. [25].

Apart from radiative corrections, another important ingredient in our results is the 3d condensate $\langle\phi^\dagger\phi\rangle_{\mathrm{3d}}$ (cf. eq. (5.14)), measured non-perturbatively on the lattice and subsequently converted to the $\overline{\mathrm{MS}}$ scheme. It is interesting to note that apart from the known strong correlation of $\langle\phi^\dagger\phi\rangle_{\mathrm{3d}}$ with the anomalous rate of baryon plus lepton number violation (cf. refs. [6, 30] and references therein), the same quantity also plays a role for other cosmologically relevant observables, such as the production rate of non-relativistic right-handed neutrinos [31] or the relationship between lepton and baryon number densities [32]. Therefore, it seems well motivated to improve on the existing measurements [6] by including the U(1) subgroup and by taking the continuum limit for a physical Higgs mass. In addition, it would be helpful to measure the susceptibility related to this condensate, so that taking a numerical temperature derivative, needed for estimating the heat capacity or the speed of sound squared, could be avoided.

Our interpolations of all thermodynamic functions shown in figure 4 can be downloaded, for a wide temperature interval, from www.laine.itp.unibe.ch/eos15/. (In these results we switch from one regime to another with a temperature gap of 15–20 GeV in between.) Despite the remaining uncertainties, we hope that these results turn out to be helpful as a background equation of state in Dark Matter or Leptogenesis computations operating in this temperature range.

Acknowledgments

We thank M. D'Onofrio, K. Rummukainen and A. Tranberg for providing us with numerical data from ref. [6]. This work was partly supported by the Swiss National Science Foundation (SNF) under grant 200021-146737.

A 3d condensate in perturbation theory

We collect here results for the $\overline{\mathrm{MS}}$ renormalized condensate $\langle\phi^\dagger\phi\rangle_{\mathrm{3d}}$ defined within the MSM effective theory and evaluated at the scale $\bar{\mu} = g_{\mathrm{M2}}^2$ (cf. eq. (5.9)).

For $\bar{m}_3^2 \gg 0$, a 3-loop perturbative expression for $\langle\phi^\dagger\phi\rangle_{\mathrm{3d}}$ can be extracted from eq. (35) of ref. [18], after subtracting the contributions containing adjoint scalar fields (the latter need

JCAP07(2015)035

to be corrected as explained in appendix B). The expression reads

$$\frac{\langle\phi^\dagger\phi\rangle_{3\mathrm{d}}(g^2_{\mathrm{M2}})}{g^2_{\mathrm{M2}}T} = -\frac{\sqrt{y}}{2\pi} + \frac{1}{(4\pi)^2}\left[6x + (3+z)\left(-\frac{\ln y}{2} - \ln 2 + \frac{1}{4}\right)\right] \\ + \frac{1}{(4\pi)^3\sqrt{y}}\left[\frac{51\ln y}{32} + \frac{61\ln 2}{16} + \frac{3\pi^2}{16} + \frac{485}{64} + x\left(\frac{9\ln y}{2} + 3\ln 2 + \frac{39}{4}\right)\right. \\ + x^2\left(-6\ln y - 24\ln 2 + \frac{3}{2}\right) + z\left(-\frac{9\ln y}{16} - \frac{27\ln 2}{8} + \frac{\pi^2}{8} + \frac{51}{32}\right) \\ \left. + z^2\left(-\frac{5\ln y}{32} - \frac{41\ln 2}{48} + \frac{\pi^2}{48} + \frac{47}{192}\right) + x\,z\left(\frac{3\ln y}{2} - 3\ln 2 + \frac{21}{4}\right)\right] + \mathcal{O}\left(\frac{1}{y}\right), \tag{A.1}$$

where

$$x \equiv \frac{\lambda_{\mathrm{M}}}{g^2_{\mathrm{M2}}}\,, \quad y \equiv \frac{\bar{m}_3^2(g^2_{\mathrm{M2}})}{g^4_{\mathrm{M2}}}\,, \quad z \equiv \frac{g^2_{\mathrm{M1}}}{g^2_{\mathrm{M2}}}\,. \tag{A.2}$$

As illustrated in figure 2 (dotted lines), the result agrees surprisingly well with lattice data as soon as $y \gtrsim 0.2$.

In the broken symmetry phase, i.e. for $\bar{m}_3^2 \ll 0$, an explicit loopwise result is available up to 2-loop level, however it shows poor convergence [29]. Therefore we make use of a numerically determined value (referred to as the "Coleman-Weinberg (CW) method") which includes a subset of higher-order corrections and has been tested against lattice simulations in refs. [21, 29]. The result is only available in the approximation $g_{\mathrm{M1}} = 0$ but the corrections originating from g_{M1} are expected to be small. A comparison with lattice data is shown in figure 2 (long-dashed line), with the low-temperature deviation expected to be reduced by a continuum extrapolation [21].

B Differences with respect to ref. [18]

Our results make use of expressions first derived in ref. [18], however there are a few technical points on which we disagree with this reference. As already discussed in the text, an important issue is that of the overall renormalization condition, eq. (2.6), which was imposed in a different form in ref. [18] (what was subtracted there was the pressure of a hypothetical zero-temperature "symmetric phase").

In addition, the following typographic errors have been detected in ref. [18]: in eq. (8), $-3g_Y^4 \to -N_{\mathrm{c}}g_Y^4$; in eq. (31), $g_s^2 \to g_s^2/(4\pi)^2$; in eq. (33), ${g'_3}^2 \to {g'_3}^4$ and $2{h'_3}^2 \to \frac{1}{2}{h'_3}^2$; on the 1st line of eq. (35), $\ln\frac{\mu_3}{2m_3} \to \ln\frac{\mu_3}{2(m_3^2+\delta m_3^2)^{1/2}}$; on the 5th row of eq. (45), $\frac{25}{72} \to \frac{25}{72}\ln$.

As far as notation goes, we have replaced $g^2 \to g_2^2$, ${g'}^2 \to g_1^2$, $g_Y^2 \to h_t^2$, $\Lambda \to \bar{\mu}$, and $\gamma \to \gamma_{\mathrm{E}}$. Because of the trickiness of hypercharge assignments for a general representation, we choose directly Standard Model group theory factors: in the notation of refs. [18, 19],

$$d_{\mathrm{F}} \to 2\,, \quad d_{\mathrm{A}} \to 3\,, \quad C_{\mathrm{F}} \to \frac{3}{4}\,, \quad C_{\mathrm{A}} \to 2\,, \quad T_{\mathrm{F}} \to \frac{1}{2}\,, \quad n_{\mathrm{S}} \to 1\,, \quad N_{\mathrm{c}} \to 3\,. \tag{B.1}$$

Only the number of fermion generations, denoted by n_{G}, is left free in our results. In order to simplify the expressions somewhat, we also substitute $h_3 \to g_2^2/4$, $h'_3 \to g_1^2/4$.

We disagree with the square brackets in eq. (198) of ref. [18]. In the notation of ref. [18], this term arises from the three-dimensional integral

$$\mathcal{I}_{\mathrm{new}} \equiv \int_{pqr} \frac{1}{(p^2+m_{\mathrm{D}}^2)[(r-p)^2+m_{\mathrm{D}}^2](q^2+m_3^2)[(r-q)^2+m_3^2]r^4}\,. \tag{B.2}$$

JCAP07(2015)035

Because of an infrared divergence, the integral needs to be carried out in the presence of dimensional regularization. The infrared divergence is powerlike so that, in the end, the limit $\epsilon \to 0$ can be taken. The square brackets in eq. (198) of ref. [18] correspond to the combination $[\ldots] \equiv 24(4\pi)^3 m_{\rm D}^2 m_3^2 \mathcal{I}_{\rm new}$, and we believe that this combination has to be replaced as

$$\begin{aligned} &\left[\frac{m_{\rm D}^2}{m_3}\ln\frac{m_3+m_{\rm D}}{m_{\rm D}}+\frac{m_3^2}{m_{\rm D}}\ln\frac{m_3+m_{\rm D}}{m_3}-4(m_3+m_{\rm D})\right] \\ \to\; &-\left[\frac{m_{\rm D}^2}{m_3}\ln\frac{m_3+m_{\rm D}}{m_{\rm D}}+\frac{m_3^2}{m_{\rm D}}\ln\frac{m_3+m_{\rm D}}{m_3}+\frac{m_3+m_{\rm D}}{2}\right]. \end{aligned} \tag{B.3}$$

Consequently, a round bracket on the third-but-last line in eq. (35) of ref. [18] needs to be changed as

$$\begin{aligned} &g_3^4 C_{\rm A} C_{\rm F} d_{\rm F} \frac{1}{3}\left(\frac{m_3^2}{m_{\rm D}}\ln\frac{m_{\rm D}+m_3}{m_3}+\frac{m_{\rm D}^2}{m_3}\ln\frac{m_{\rm D}+m_3}{m_{\rm D}}\right) \\ \to\; &g_3^4 C_{\rm A} C_{\rm F} d_{\rm F} \frac{1}{6}\left(\frac{m_3^2}{m_{\rm D}}\ln\frac{m_{\rm D}+m_3}{m_3}+\frac{m_{\rm D}^2}{m_3}\ln\frac{m_{\rm D}+m_3}{m_{\rm D}}+\frac{7}{4}\,(m_{\rm D}+m_3)\right). \end{aligned} \tag{B.4}$$

References

[1] K. Kajantie, M. Laine, K. Rummukainen and M.E. Shaposhnikov, *Is there a hot electroweak phase transition at $m_H \gtrsim m_W$?*, *Phys. Rev. Lett.* **77** (1996) 2887 [hep-ph/9605288] [INSPIRE].

[2] F. Karsch, T. Neuhaus, A. Patkós and J. Rank, *Critical Higgs mass and temperature dependence of gauge boson masses in the* SU(2) *gauge Higgs model*, *Nucl. Phys. Proc. Suppl.* **53** (1997) 623 [hep-lat/9608087] [INSPIRE].

[3] Y. Aoki, *Four-dimensional simulation of the hot electroweak phase transition with the* SU(2) *gauge Higgs model*, *Phys. Rev.* **D 56** (1997) 3860 [hep-lat/9612023] [INSPIRE].

[4] M. Gürtler, E.-M. Ilgenfritz and A. Schiller, *Where the electroweak phase transition ends*, *Phys. Rev.* **D 56** (1997) 3888 [hep-lat/9704013] [INSPIRE].

[5] M. Laine and K. Rummukainen, *What's new with the electroweak phase transition?*, *Nucl. Phys. Proc. Suppl.* **73** (1999) 180 [hep-lat/9809045] [INSPIRE].

[6] M. D'Onofrio, K. Rummukainen and A. Tranberg, *Sphaleron Rate in the Minimal Standard Model*, *Phys. Rev. Lett.* **113** (2014) 141602 [arXiv:1404.3565] [INSPIRE].

[7] L. Canetti, M. Drewes, T. Frossard and M. Shaposhnikov, *Dark Matter, Baryogenesis and Neutrino Oscillations from Right Handed Neutrinos*, *Phys. Rev.* **D 87** (2013) 093006 [arXiv:1208.4607] [INSPIRE].

[8] G. Steigman, B. Dasgupta and J.F. Beacom, *Precise Relic WIMP Abundance and its Impact on Searches for Dark Matter Annihilation*, *Phys. Rev.* **D 86** (2012) 023506 [arXiv:1204.3622] [INSPIRE].

[9] M. Hindmarsh and O. Philipsen, *WIMP dark matter and the QCD equation of state*, *Phys. Rev.* **D 71** (2005) 087302 [hep-ph/0501232] [INSPIRE].

[10] M. Drees, F. Hajkarim and E.R. Schmitz, *The Effects of QCD Equation of State on the Relic Density of WIMP Dark Matter*, *JCAP* **06** (2015) 025 [arXiv:1503.03513] [INSPIRE].

[11] P.H. Ginsparg, *First Order and Second Order Phase Transitions in Gauge Theories at Finite Temperature*, *Nucl. Phys.* **B 170** (1980) 388 [INSPIRE].

[12] T. Appelquist and R.D. Pisarski, *High-Temperature Yang-Mills Theories and Three-Dimensional Quantum Chromodynamics*, *Phys. Rev.* **D 23** (1981) 2305 [INSPIRE].

JCAP07(2015)035

[13] K. Kajantie, M. Laine, K. Rummukainen and M.E. Shaposhnikov, *Generic rules for high temperature dimensional reduction and their application to the Standard Model*, *Nucl. Phys.* **B 458** (1996) 90 [hep-ph/9508379] [INSPIRE].

[14] A.D. Linde, *Infrared Problem in Thermodynamics of the Yang-Mills Gas*, *Phys. Lett.* **B 96** (1980) 289 [INSPIRE].

[15] D.J. Gross, R.D. Pisarski and L.G. Yaffe, *QCD and Instantons at Finite Temperature*, *Rev. Mod. Phys.* **53** (1981) 43 [INSPIRE].

[16] F. Csikor, Z. Fodor and J. Heitger, *Endpoint of the hot electroweak phase transition*, *Phys. Rev. Lett.* **82** (1999) 21 [hep-ph/9809291] [INSPIRE].

[17] M. Laine, *The renormalized gauge coupling and non-perturbative tests of dimensional reduction*, *JHEP* **06** (1999) 020 [hep-ph/9903513] [INSPIRE].

[18] A. Gynther and M. Vepsäläinen, *Pressure of the standard model at high temperatures*, *JHEP* **01** (2006) 060 [hep-ph/0510375] [INSPIRE].

[19] A. Gynther and M. Vepsäläinen, *Pressure of the standard model near the electroweak phase transition*, *JHEP* **03** (2006) 011 [hep-ph/0512177] [INSPIRE].

[20] E. Braaten and A. Nieto, *Free energy of QCD at high temperature*, *Phys. Rev.* **D 53** (1996) 3421 [hep-ph/9510408] [INSPIRE].

[21] M. D'Onofrio, K. Rummukainen and A. Tranberg, *The Sphaleron Rate through the Electroweak Cross-over*, *JHEP* **08** (2012) 123 [arXiv:1207.0685] [INSPIRE].

[22] A.K. Rajantie, *Feynman diagrams to three loops in three-dimensional field theory*, *Nucl. Phys.* **B 480** (1996) 729 [*Erratum ibid.* **B 513** (1998) 761] [hep-ph/9606216] [INSPIRE].

[23] P. Giovannangeli, *Two loop renormalization of the magnetic coupling in hot QCD*, *Phys. Lett.* **B 585** (2004) 144 [hep-ph/0312307] [INSPIRE].

[24] M. Laine and A. Rajantie, *Lattice continuum relations for* 3*d* SU(N) + *Higgs theories*, *Nucl. Phys.* **B 513** (1998) 471 [hep-lat/9705003] [INSPIRE].

[25] M. Laine and Y. Schröder, *Quark mass thresholds in QCD thermodynamics*, *Phys. Rev.* **D 73** (2006) 085009 [hep-ph/0603048] [INSPIRE].

[26] K. Kajantie, M. Laine, K. Rummukainen and Y. Schröder, *The pressure of hot QCD up to* $g^6 ln(1/g)$, *Phys. Rev.* **D 67** (2003) 105008 [hep-ph/0211321] [INSPIRE].

[27] S. Borsányi, G. Endrődi, Z. Fodor, S.D. Katz and K.K. Szabó, *Precision* SU(3) *lattice thermodynamics for a large temperature range*, *JHEP* **07** (2012) 056 [arXiv:1204.6184] [INSPIRE].

[28] J. Ignatius, K. Kajantie, H. Kurki-Suonio and M. Laine, *Large scale inhomogeneities from the QCD phase transition*, *Phys. Rev.* **D 50** (1994) 3738 [hep-ph/9405336] [INSPIRE].

[29] K. Kajantie, M. Laine, K. Rummukainen and M.E. Shaposhnikov, *The electroweak phase transition: A nonperturbative analysis*, *Nucl. Phys.* **B 466** (1996) 189 [hep-lat/9510020] [INSPIRE].

[30] V.A. Kuzmin, V.A. Rubakov and M.E. Shaposhnikov, *On the Anomalous Electroweak Baryon Number Nonconservation in the Early Universe*, *Phys. Lett.* **B 155** (1985) 36 [INSPIRE].

[31] M. Laine and Y. Schröder, *Thermal right-handed neutrino production rate in the non-relativistic regime*, *JHEP* **02** (2012) 068 [arXiv:1112.1205] [INSPIRE].

[32] D. Bödeker and M. Sangel, *Order* g^2 *susceptibilities in the symmetric phase of the Standard Model*, *JCAP* **04** (2015) 040 [arXiv:1501.03151] [INSPIRE].

JCAP07(2015)035